tion ($\omega \approx \omega_0$). Also determine the peak values of χ_e'' and their locations with respect to ω_0.

1.10. Consider two waves having different frequencies, ω_1 and ω_2, that propagate in opposite directions along the z axis. Show that the resulting "standing wave" field distribution moves along the z axis at a velocity proportional to the frequency difference.

REFERENCES

1. S. Ramo, J. R. Whinnery, and T. Van Duzer, *Fields and Waves in Communication Electronics*, 3rd ed. Wiley, New York, 1994.
2. F. A. Jenkins and H. E. White, *Fundamentals of Optics*. McGraw-Hill, New York, 1976.
3. E. Hecht and A. Zajac, *Optics*. Addison-Wesley, Menlo Park, CA, 1979.
4. D. K. Cheng, *Field and Wave Electromagnetics*, 2nd ed. Addison-Wesley, Reading, MA, 1989.
5. J. D. Kraus, *Electromagnetics*, 4th ed. McGraw-Hill, New York, 1991.

2

Symmetric Dielectric Slab Waveguides

As a first step in the study of optical waveguides, the light-guiding properties of the dielectric slab waveguide are presented in this chapter. This structure is of great importance in the area of integrated optics, where it is a basic component in the construction of many devices. The properties of the guide (field configuration, behavior with frequency, etc.) are qualitatively similar to the optical fiber but are simpler and more easily understood. The special case of symmetric geometry, having equal refractive indices above and below the guiding layer, is presented here. The analysis of nonsymmetric structures is similar and is covered in other texts [1,2].

The symmetric slab geometry is shown in Fig. 2.1. The guide is assumed infinite in the y direction, implying that no electromagnetic quantity will vary in this direction. Three lossless dielectric regions comprise the structure. The middle layer, known as the *slab* or *film*, is of thickness d and has refractive index n_1, where $n_1 > n_2$. The upper and lower regions, having index n_2, are semi-infinite in the positive and negative x directions. The permeability in all regions is assumed to be that of free space, μ_0. Light is launched into the slab from the left, and the resulting guided modes propagate in the positive z direction.

2.1. RAY ANALYSIS OF THE SLAB WAVEGUIDE

It is possible to analyze the waveguide modes as superpositions of plane waves that propagate in zigzag paths characterized by *rays*. This approach is easiest to implement in media having boundaries that extend over distances very large compared to a wavelength, and in which local index variations are very small over distances comparable to a wavelength. Light rays are confined within the structure by the mechanism of total reflection at the interfaces. This will occur if $\theta_1 \geq \theta_c$. where θ_1 is the ray angle measured with respect to the normal to the interface, and θ_c is the critical angle, given by $\sin\theta_c = n_2/n_1$. It is apparent that this condition can be satisfied only if $n_1 > n_2$.

Figure 2.1 shows a single ray propagating in a zigzag path, reflecting from both interfaces at angle θ_1. Associated with this ray are two plane waves. One propagates along the upward path with wavevector $\mathbf{k}_u$; the other propagates along the downward path with wavevector $\mathbf{k}_d$. The two vectors are expressed in terms of their cartesian components as

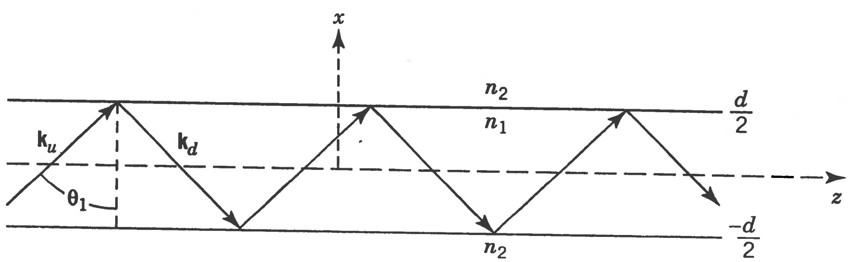

Figure 2.1. Symmetric slab ray geometry.

To achieve a propagating mode, it is necessary that the wavefronts associated with the first upward propagating ray be exactly coincident with those of all subsequent upward rays. The net upward propagating power will thus be in the form of a single plane wave. A similar requirement holds for the downward rays. If the above conditions are not satisfied, then the composite wave (or mode) will not propagate, since destructive interference would occur between the various reflected components. For a given wavelength, guide thickness, and choice of indices, only certain values of θ_1 will satisfy the requirement. Each allowed θ_1 value corresponds to a single mode of the guide.

Two distinct mode types can exist, depending on the orientation of the electric and magnetic fields of the plane waves. Figure 2.2 shows the two types. With the electric field polarized in the xz plane, the magnetic field lies entirely in the transverse plane (along the y axis), forming a transverse magnetic (or TM) mode. The opposite case occurs when **H** lies in the xz plane, leaving **E** in the transverse plane, resulting in a transverse electric (or TE) mode.

The upward and downward propagating fields are expressed in the standard phasor form, shown here for a single component of **E**:

$$E_u = E_0 \exp(-j\mathbf{k}_u \cdot \mathbf{r}) = E_0 \exp(-jk_{x1}x)\exp(-j\beta z) \tag{2.1}$$

$$E_d = E_0 \exp(-j\mathbf{k}_d \cdot \mathbf{r}) = E_0 \exp(+jk_{x1}x)\exp(-j\beta z) \tag{2.2}$$

where $\mathbf{r} = x\hat{\mathbf{a}}_x + z\hat{\mathbf{a}}_z$. The wavevector magnitudes are $|\mathbf{k}_u| = |\mathbf{k}_d| = k_1 = n_1 k_0$. The

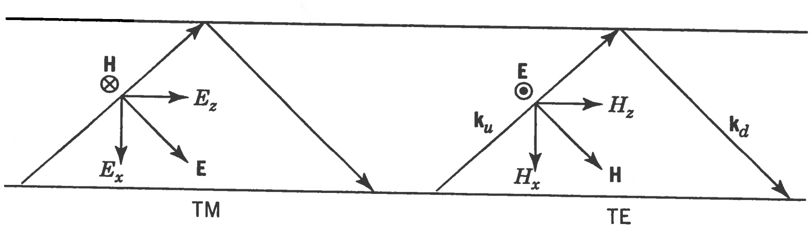

Figure 2.2. The two types of slab waveguide modes.

wavevector component magnitudes are expressed as

$$k_{x1} = k_1 \cos\theta_1 = n_1 k_0 \cos\theta_1 \tag{2.3}$$

and

$$\beta = k_1 \sin\theta_1 = n_1 k_0 \sin\theta_1 \tag{2.4}$$

where $k_0 \equiv \omega\sqrt{\mu_0\epsilon_0} = 2\pi/\lambda$ is the free-space propagation constant, and λ is the wavelength of light measured in vacuum. The z component of either wavevector, β (also the mode propagation constant), is one of the quantities that is necessary to determine for each mode of a guide. From β, the mode phase velocity (ω/β) and group velocity ($d\omega/d\beta$) can be found. The dependence of the latter quantity on frequency enables the evaluation of signal distortion that will occur in a given mode. It is clear that, at a given frequency, different modes will have different values of β and may consequently have different group velocities. Hence, in a multimode guide, in which an appreciable fraction of the signal power is carried in each mode, the different propagation times of the modes may produce severe signal distortion. For this reason, a guide that propagates light in a single mode is preferable.

To study the wave reflection process, the possibility of propagating fields above and below the slab must be included. To see this, consider the "leaky" wave case shown in Fig. 2.3. In it, reflection of a slab ray at each interface results in partial transmission into the upper and lower regions. The wavevectors of the transmitted rays are of magnitude k_2. Considering the upper region ($x \geq d/2$), $\mathbf{k}_2$ is projected into x and z components, k_{x2} and β, respectively. The z components of $\mathbf{k}_1$ and $\mathbf{k}_2$ must be equal to enable the field boundary conditions to be satisfied at all positions along the interface at all times. The transmitted wavevectors in the lower region ($x \leq -d/2$) are projected in a similar way, resulting in x- and z-component magnitudes that are identical to those found in the upper region.

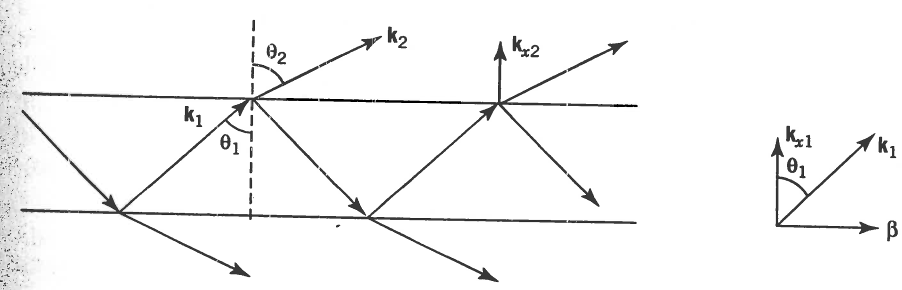

Figure 2.3. Wavevector geometries at the interfaces.

It is necessary to determine (1) the relationship between the ray angles, θ_1 and θ_2, and the refractive indices and (2) the relationship between the incident and reflected wave amplitudes. The first relationship is given by Snell's law: $n_1 \sin\theta_1 = n_2 \sin\theta_2$. The amplitude relationship is found through the Fresnel equations, (1.44) and (1.46), providing reflection coefficients:

$$\Gamma_{\mathrm{TE}} = \frac{k_{x1} - k_{x2}}{k_{x1} + k_{x2}} = \frac{n_1 \cos\theta_1 - n_2 \cos\theta_2}{n_1 \cos\theta_1 + n_2 \cos\theta_2} \tag{2.5}$$

$$\Gamma_{\mathrm{TM}} = \frac{n_2^2 k_{x1} - n_1^2 k_{x2}}{n_2^2 k_{x1} + n_1^2 k_{x2}} = \frac{n_2 \sec\theta_2 - n_1 \sec\theta_1}{n_2 \sec\theta_2 + n_1 \sec\theta_1} \tag{2.6}$$

To achieve a completely guided mode, the waves must be totally reflected at both interfaces; that is, the magnitudes of Γ_{TE} (or Γ_{TM}) will be unity. As explained in Chapter 1, total reflection will occur when $\theta_1 \geq \theta_c$.

An electric field component in the upper region will assume the phasor form:

$$E_2 = E_{20} \exp(-j\mathbf{k}_2 \cdot \mathbf{r}) = E_{20} \exp(-jk_{x2}x) \exp(-j\beta z) \tag{2.7}$$

When the critical angle is exceeded in the slab, k_{x2} becomes imaginary and can be expressed in terms of a real attenuation coefficient as

$$k_{x2} = -j\gamma_2 \qquad \theta_1 > \theta_c \tag{2.8}$$

E_2 now becomes $E_2 = E_{20} \exp(-\gamma_2 x) \exp(-j\beta z)$. This is the phasor expression for a *surface* or *evanescent* wave, which propagates only in the z direction and which decreases in amplitude as the magnitude of x increases in the upper and lower regions. Using Snell's law, γ_2 can be expressed as

$$\gamma_2 = jk_{x2} = jn_2 k_0 \cos\theta_2 = jn_2 k_0 (-j) \left[\left(\frac{n_1}{n_2} \right)^2 \sin^2\theta_1 - 1 \right]^{1/2}$$
$$= (\beta^2 - n_2^2 k_0^2)^{1/2} \tag{2.9}$$

Note that large θ_1 implies large γ_2, leading to tighter confinement of the wave within the slab. Inside the slab, the wavevector components obey the relation $k_1^2 = n_1^2 k_0^2 = k_{x1}^2 + \beta^2$. Therefore

$$k_{x1} = (n_1^2 k_0^2 - \beta^2)^{1/2} \tag{2.10}$$

For a wave to be completely guided (no radiation leakage), k_{x1} and γ_2 must both be real. Using (2.8) and (2.10), we observe that the values of β for a completely guided wave are confined to the range

$$n_2 k_0 < \beta < n_1 k_0 \tag{2.11}$$

Recall that phase velocity is $v_p = \omega/\beta$ and $k_0 = \omega/c$. Using these in (2.11) results in

$$\frac{c}{n_1} < v_p < \frac{c}{n_2} \tag{2.12}$$

as the allowed range of phase velocities for a guided mode.

With the total reflection condition established, the plane wave will experience a phase shift on reflection, 2ϕ, which will be a function of θ_1. Considering the TE case with total reflection, we see that (2.5) becomes

$$\Gamma_{\mathrm{TE}} = \frac{k_{x1} + j\gamma_2}{k_{x1} - j\gamma_2} \tag{2.13}$$

By defining $Z = k_{x1} + j\gamma_2$, (2.13) becomes $\Gamma_{\mathrm{TE}} = Z/Z^* = \exp(j2\phi_{\mathrm{TE}})$, where

$$\phi_{\mathrm{TE}} = \tan^{-1}\left(\frac{\gamma_2}{k_{x1}} \right) = \tan^{-1}\left(\frac{(n_1^2 \sin^2\theta_1 - n_2^2)^{1/2}}{n_1 \cos\theta_1} \right) \tag{2.14}$$

In a similar manner, it can be shown that, for the TM case,

$$\phi_{\mathrm{TM}} = \tan^{-1}\left(\frac{n_1^2}{n_2^2} \frac{(n_1^2 \sin^2\theta_1 - n_2^2)^{1/2}}{n_1 \cos\theta_1} \right) \tag{2.15}$$

From (2.14) and (2.15) it is observed that ϕ_{TE} and ϕ_{TM} will increase from 0 to $\pi/2$ as θ_1 increases from θ_c to $\pi/2$.

The eigenvalue equations for the propagating modes can now be derived. The requirement is that all upward propagating plane waves in the guide must be precisely in phase (the same is true for all downward propagating waves). Consider one complete "bounce" of a slab ray, consisting of two traversals of the slab and two reflections. The above condition will be satisfied if the net *transverse* phase shift of the wave over this path is an integer multiple of 2π (it is helpful to use appropriate sketches of the propagating phase fronts to illustrate this fact). Consider a starting electric field value, E_s, and its value at the end of a complete round trip, E_f. The two are related by

$$E_f = E_s \exp(-jk_{x1}d) \exp(j2\phi) \exp(-jk_{x1}d) \exp(j2\phi) \tag{2.16}$$

where ϕ is either ϕ_{TE} or ϕ_{TM}, as appropriate. To achieve self-consistency, $E_s = E_f$, resulting in the *transverse resonance condition:*

$$4\phi - 2k_{x1}d = 2m\pi \tag{2.17}$$

where m, an integer, is called the mode number or rank. For TE waves, (2.14) and (2.17) are used to obtain

$$\tan^{-1}\left(\frac{\gamma_2}{k_{x1}}\right) = \frac{k_{x1}d}{2} + \frac{m\pi}{2} \tag{2.18}$$

or

$$\frac{\gamma_2}{k_{x1}} = \tan\left(\frac{k_{x1}d}{2} + \frac{m\pi}{2}\right) = \begin{cases} \tan\left(\dfrac{k_{x1}d}{2}\right) & m = 0, 2, 4, \ldots \\ -\cot\left(\dfrac{k_{x1}d}{2}\right) & m = 1, 3, 5, \ldots \end{cases} \tag{2.19}$$

A similar procedure is carried out for the TM case. Collecting results, the following four eigenvalue equations are obtained:

$$\text{even TE:} \quad \frac{\gamma_2}{k_{x1}} = \tan\left(\frac{k_{x1}d}{2}\right) \qquad m = 0, 2, 4, \ldots \tag{2.20}$$

$$\text{odd TE:} \quad \frac{\gamma_2}{k_{x1}} = -\cot\left(\frac{k_{x1}d}{2}\right) \qquad m = 1, 3, 5, \ldots \tag{2.21}$$

$$\text{even TM:} \quad \frac{\gamma_2}{k_{x1}} = \frac{n_2^2}{n_1^2}\tan\left(\frac{k_{x1}d}{2}\right) \qquad m = 0, 2, 4, \ldots \tag{2.22}$$

$$\text{odd TM:} \quad \frac{\gamma_2}{k_{x1}} = -\frac{n_2^2}{n_1^2}\cot\left(\frac{k_{x1}d}{2}\right) \qquad m = 1, 3, 5, \ldots \tag{2.23}$$

These transcendental equations must be solved graphically or numerically for γ_2 and k_{x1}. β can then be found using (2.10). A graphical technique for their solution is presented in Section 2.4.

2.2. FIELD ANALYSIS OF THE SLAB WAVEGUIDE

In the last section, the eigenvalue equations for the slab waveguide modes were obtained without any direct use of the actual field configurations. In fact, the

equations to obtain the condition for total reflection, in addition to the phase shifts of the reflected rays. In this section, the slab mode fields are found by solving the wave equation. It is then shown how the eigenvalue equations are determined by applying appropriate boundary conditions for the fields at the guide interfaces.

The analysis begins by assuming an electric field solution of the form

$$\mathbf{E}(x, z) = \mathbf{E}_0(x)\exp(-j\beta z) \tag{2.24}$$

where $\mathbf{E}_0(x)$ is to be determined. The wave equation is used, which, for a general z-propagating sinusoidal field, assumes the form given by (1.21):

$$\nabla_t^2\mathbf{E}_0(x, y) + (k^2 - \beta^2)\mathbf{E}_0(x, y) = 0 \tag{2.25}$$

where ∇_t^2 is the Laplacian taken over x and y only. In cartesian coordinates, (2.25) will separate into individual equations for each component of $\mathbf{E}_0$. In the present case, TM waves will be considered; the z component of $\mathbf{E}_0$ will be found. Since $k^2 - \beta^2 = k_x^2$, and since there is no y variation, (2.25) simplifies to the following expression that is valid inside the slab:

$$\frac{d^2E_{z1}}{dx^2} + k_{x1}^2E_{z1} = 0 \tag{2.26}$$

Above and below the slab, $k_x = k_{x2} = -j\gamma_2$ and, as a result,

$$\frac{d^2E_{z2}}{dx^2} - \gamma_2^2E_{z2} = 0 \tag{2.27}$$

The solution of (2.26) is:

$$E_{z1}(x, z) = [E_e\sin(k_{x1}x) + E_o\cos(k_{x1}x)]\exp(-j\beta z) \qquad \frac{-d}{2} \le x \le \frac{d}{2} \tag{2.28}$$

where E_e and E_o are the field amplitudes for the cases of even and odd mode number, m, as will be seen later. E_{z1} is seen to be a standing wave in x, characterized by spatial frequency k_{x1} in that direction. The field pattern propagates in the forward z direction with propagation constant β.

The solution of (2.27) is a pair of evanescent waves, existing above and

$$E_{z2}(x,z) = \begin{cases} E_c \exp[-\gamma_2(x - d/2)]\exp(-j\beta z) & x \geq d/2 \\ \pm E_c \exp[+\gamma_2(x + d/2)]\exp(-j\beta z) & x \leq -d/2 \end{cases} \tag{2.29}$$

The field amplitude, E_c, is found in terms of E_e and E_o by applying the boundary condition of continuous tangential electric field at each interface:

$$E_{z1}(x = \pm d/2) = E_{z2}(x = \pm d/2) \tag{2.30}$$

The choice of either sine or cosine for the x dependence of E_{z1} provides two separate cases for the TM modes. Consider first the choice of the sine dependence, which will be called *Case I TM*:

$$E^{I}_{z1}(x,z) = E_e \sin(k_{x1}x)\exp(-j\beta z) \tag{2.31}$$

Applying (2.30) and using (2.29) results in $E_c = E_e \sin(k_{x1}d/2)$. Outside the slab, the field for Case I TM then assumes the form

$$E^{I}_{z2}(x,z) = \begin{cases} E_e \sin(k_{x1}d/2)\exp[-\gamma_2(x - d/2)]\exp(-j\beta z) & x \geq d/2 \\ -E_e \sin(k_{x1}d/2)\exp[+\gamma_2(x + d/2)]\exp(-j\beta z) & x \leq -d/2 \end{cases} \tag{2.32}$$

The minus sign is chosen for the $x \leq -d/2$ field, since $\sin(k_{x1}x)$ changes sign at $x = 0$.

The other possibility is called *Case II TM*:

$$E^{II}_{z1}(x,z) = E_o \cos(k_{x1}x)\exp(-j\beta z) \tag{2.33}$$

Equations (2.29) and (2.30) are used with (2.33) to obtain

$$E^{II}_{z2}(x,z) = \begin{cases} E_o \cos(k_{x1}d/2)\exp[-\gamma_2(x - d/2)]\exp(-j\beta z) & x \geq d/2 \\ E_o \cos(k_{x1}d/2)\exp[+\gamma_2(x + d/2)]\exp(-j\beta z) & x \leq -d/2 \end{cases} \tag{2.34}$$

A similar procedure can be carried out for TE waves, in which the wave equation is solved for H_z instead of E_z. The steps involved are nearly identical to the above, the major exception being that tangential continuity of H across an interface is used to evaluate constants. Inside the slab, H_z assumes a sine (Case I) or a cosine (Case II) form, in analogy to E_z. The details of the wave

Having the z components of **E** inside and outside the slab, the transver components remain to be found. This is accomplished in a straightforward ma ner using Maxwell's equations. The two curl equations, assuming sourcele media, take the form

$$\nabla \times \mathbf{E} = -j\omega\mu\mathbf{H} \tag{2.3}$$

and

$$\nabla \times \mathbf{H} = j\omega\epsilon\mathbf{E} \tag{2.36}$$

Equations (2.35) and (2.36) can each be separated into three components. Fo example,

$$(\nabla \times \mathbf{E})_x = \left(\frac{\partial E_z}{\partial y} - \frac{\partial E_y}{\partial z}\right) = -j\omega\mu H_x, \text{ etc.}$$

where $\partial/\partial z = -j\beta$. Continuing this procedure results in a set of six equation representing the individual components of (2.35) and (2.36):

$$\frac{\partial E_z}{\partial y} + j\beta E_y = -j\omega\mu H_x \tag{2.35a}$$

$$\frac{\partial E_z}{\partial x} + j\beta E_x = j\omega\mu H_y \tag{2.35b}$$

$$\frac{\partial E_y}{\partial x} - \frac{\partial E_x}{\partial y} = -j\omega\mu H_z \tag{2.35c}$$

$$\frac{\partial H_z}{\partial y} + j\beta H_y = j\omega\epsilon E_x \tag{2.36a}$$

$$\frac{\partial H_z}{\partial x} + j\beta H_x = -j\omega\epsilon E_y \tag{2.36b}$$

$$\frac{\partial H_y}{\partial x} - \frac{\partial H_x}{\partial y} = j\omega\epsilon E_z \tag{2.36c}$$

Using (2.35a), (2.35b), (2.36a), and (2.36b), it is possible to obtain expressions for individual transverse components in terms of derivatives of z components. For example, E_y can be eliminated between (2.35a) and (2.36b) to obtain

$$H_x = -\frac{1}{k_x^2}\left(j\beta\frac{\partial H_z}{\partial x} - j\omega\epsilon\frac{\partial E_z}{\partial y}\right) \tag{2.37}$$

equations for the remaining three transverse components are found:

$$H_y = -\frac{1}{k_x^2}\left(j\beta \frac{\partial H_z}{\partial y} + j\omega\epsilon \frac{\partial E_z}{\partial x}\right) \tag{2.38}$$

$$E_x = -\frac{1}{k_x^2}\left(j\beta \frac{\partial E_z}{\partial x} + j\omega\mu \frac{\partial H_z}{\partial y}\right) \tag{2.39}$$

$$E_y = -\frac{1}{k_x^2}\left(j\beta \frac{\partial E_z}{\partial y} - j\omega\mu \frac{\partial H_z}{\partial x}\right) \tag{2.40}$$

As an example, the y component of **H** can be found. Using (2.38) (with E_z only) results in

$$\begin{aligned} H_y &= -\frac{1}{k_x^2}\left(j\omega\epsilon \frac{\partial E_z}{\partial x}\right) \\ &= \begin{cases} -(1/k_{x1}^2)(j\omega\epsilon_0 n_1^2\, \partial E_{z1}/\partial x) & -d/2 \le x \le d/2 \\ (1/\gamma_2^2)(j\omega\epsilon_0 n_2^2\, \partial E_{z2}/\partial x) & x \ge d/2 \text{ and } x \le -d/2 \end{cases} \end{aligned} \tag{2.41}$$

For Case I TM, it is found that

$$H_{y1}^I(x,z) = \frac{-j\omega\epsilon_0 n_1^2}{k_{x1}} E_e \cos(k_{x1}x)\exp(-j\beta z) \tag{2.42}$$

and

$$H_{y2}^I(x,z) = \begin{cases} \dfrac{-j\omega\epsilon_0 n_2^2}{\gamma_2} E_e \sin(k_{x1}d/2)\exp[-\gamma_2(x - d/2)]\exp(-j\beta z) \\ \qquad x \ge d/2 \\ \dfrac{-j\omega\epsilon_0 n_2^2}{\gamma_2} E_e \sin(k_{x1}d/2)\exp[+\gamma_2(x + d/2)]\exp(-j\beta z) \\ \qquad x \le -d/2 \end{cases} \tag{2.43}$$

The requirement of tangential continuity of **H** across an interface is now used, which in the present case becomes

$$H_{y1}^I(x = \pm d/2) = H_{y2}^I(x = \pm d/2) \tag{2.44}$$

Substitution of (2.42) and (2.43) into (2.44) leads directly to the eigenvalue equation, (2.22). It is thus seen that Case I corresponds to even values of mode

number, m, whereas the Case II solutions will be found to be associated wi odd m. Each of Eqs. (2.20) through (2.23) can be derived using procedur similar to that shown above.

2.3. SOLUTIONS OF THE EIGENVALUE EQUATIONS

The solutions of (2.20) through (2.23) are now addressed. It will be found th for each value of m (and for a fixed guide configuration and wavelength), ther is a single value of k_{x1} and a single value of β for each of the two mode type (TE and TM). k_{x1} increases as m increases, whereas β decreases. Also, for given value of m, k_{x1} and β will vary with wavelength, slab thickness, and th refractive indices.

Equations (2.20) through (2.23) are best solved numerically. On the othe hand, the use of a graphical method, while not as accurate, provides a usefu illustration of mode behavior. The graphical method presented here uses the x directed propagation and attenuation constants, k_{x1} and γ_2, that are normalize with respect to the slab thickness, d. By using (2.9) and (2.10), it is found tha

$$(k_{x1}d)^2 + (\gamma_2 d)^2 = k_0^2 d^2(n_1^2 - n_2^2) \tag{2.45}$$

When plotted with coordinate axes, $k_{x1}d$ and $\gamma_2 d$, (2.45) is the equation of circle of radius

$$R = k_0 d(n_1^2 - n_2^2)^{1/2} \tag{2.46}$$

Solving (2.45) for $\gamma_2 d$ and using (2.20) and (2.21) lead to

$$\gamma_2 d = d[k_0^2(n_1^2 - n_2^2) - k_{x1}^2]^{1/2} = \begin{cases} k_{x1}d\tan(k_{x1}d/2) & m = 0,2,4,\ldots \\ -k_{x1}d\cot(k_{x1}d/2) & m = 1,3,5,\ldots \end{cases} \tag{2.47}$$

for TE modes. The above is plotted in Fig. 2.4. Note that the tangent and cotangent curves get steeper with branch number, since each is multiplied by $k_{x1}d$. The intersections of the circle with the branches determine solutions (values of k_{x1} and γ_2) of (2.47).

Several facts can be observed from Fig. 2.4.

1. From (2.46) it is seen that an increase in frequency, index difference, or slab thickness will increase the value of R, leading to additional solutions and thus the possibility of exciting more modes.

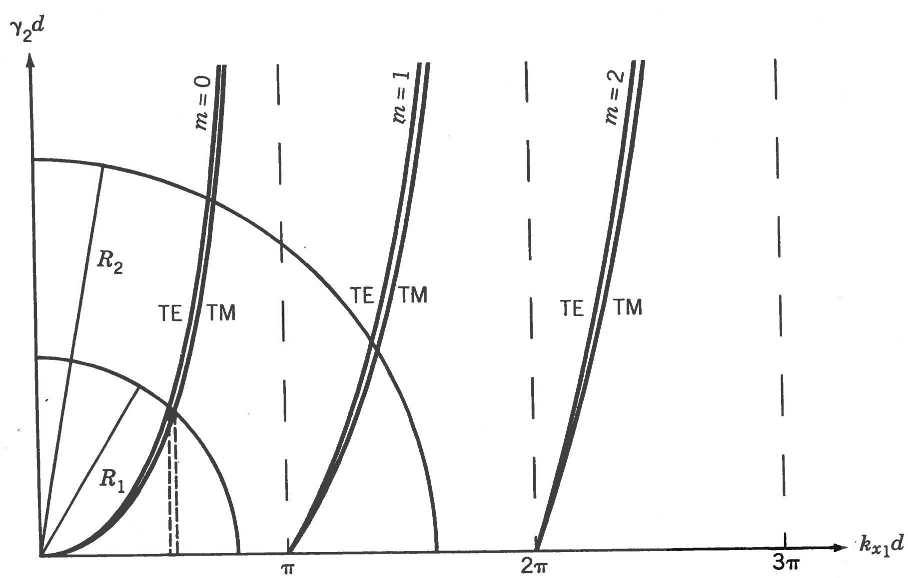

Figure 2.4. Plot of a graphical solution for TE and TM modes in a symmetric slab waveguide, showing the single-mode (R_1) and multimode (R_2) cases. Note that the TE and TM modes that are associated with a given value of m are nearly degenerate, meaning that their k_{x1} and β values are nearly equal.

2. Cutoff for a mode of mode number m occurs when $R = m\pi$. At this value:
   a. The cutoff frequency can be determined from the above to be

$$f_c = \frac{\omega_c}{2\pi} = \frac{mc}{2d(n_1^2 - n_2^2)^{1/2}} \tag{2.48}$$

   where c is the velocity of light. At frequencies less than f_c, the mode will not propagate.
   b. The value of γ_2 is zero, indicating no confinement for the mode.
   c. The ray angle, θ_1, can be shown to be equal to the critical angle, θ_c.
3. There is no cutoff for an $m = 0$ mode.
4. At a given frequency, k_{x1} is larger and θ_1 is less for higher order modes (recall that $k_{x1} = n_1 k_0 \cos\theta_1$).
5. At a given frequency, γ_2 is greater for lower order modes. As a result, these are more tightly confined to the slab.

Figure 2.4 depicts a graphical solution for TE and TM modes. Including the TM modes introduces an additional set of tangent and cotangent curves that are slightly offset from the TE curves as shown; the offset arises from the added

factor of n_2^2/n_1^2 from (2.23) and (2.24). Each value of m therefore correspond to a pair of modes, TE_m and TM_m, which will have propagation constants th differ slightly. It is thus impossible to obtain a truly single-mode symmetri slab guide by lowering the frequency to obtain $m = 0$ only.

A final point concerns the behavior of a given mode with frequency. Refe ring again to Fig. 2.4, note that two circles are shown, where R_2 could b said to differ from R_1 by a simple increase in frequency. R will increase lin early with frequency, whereas it is seen that $k_{x1}d$ (two values of which ar shown here for the $m = 0$ mode pair) will increase at a slower rate. Noting tha $k_{x1} = n_1 k_0 \cos\theta_1$, we see that a linear increase in frequency (k_0) must there fore be accompanied by a *decrease* in $\cos\theta_1$ in order to achieve this behavio Consequently, for a given mode, θ_1 will *increase* with frequency. Since β = $n_1 k_0 \sin\theta_1$, it is found that the phase velocity—$v_p = \omega/\beta = c/(n_1 \sin\theta_1)$—wil therefore decrease as frequency increases.

2.4. POWER TRANSMISSION AND CONFINEMENT

An important attribute of any waveguide is the amount of power transmitte through it, and the manner in which the power is distributed within the structure In dielectric guides, the existence of fields outside the slab region can result i outside objects affecting power transmission. These effects are minimized if th mode field amplitudes at the object location are as small as possible, a conditio achieved if the outer fields exhibit rapid exponential decay in x. On the othe hand, in device applications involving slab waveguides, the evanescent powe in the cladding region is typically used for input and output coupling, as wel as to enable the guided power to interact with other components that can be conveniently placed on top of the slab structure. In the case of optical fibers, knowledge of the power distribution is of critical importance for minimizing losses and for optimizing input and output coupling efficiencies. These issues will be addressed in later chapters.

Power computation begins with the time-average power density as expressed in (1.24):

$$\langle \mathbf{S} \rangle = \tfrac{1}{2}\,\mathrm{Re}\,\{\mathbf{E} \times \mathbf{H}^*\} \quad \mathrm{W/m^2} \tag{2.49}$$

where $\mathbf{S}$ is the Poynting vector, and where the electric and magnetic fields are in phasor form. The average power that is guided by the slab waveguide will be the integral of the z component of $\mathbf{S}$ over the guide transverse cross section. The general expression for the power will thus be

$$P = \int_{-\infty}^{\infty}\int_{-\infty}^{\infty} \langle \mathbf{S} \rangle \cdot \hat{\mathbf{a}}_z \, dx\, dy \quad \mathrm{W} \tag{2.50}$$